Published as: *Dev Dyn*. 2012 December ; 241(12): 1911–1921.

Functional Redundancy Between Cdc14 Phosphatases in Zebrafish Ciliogenesis

Aurélie Clément[1], **Lilianna Solnica-Krezel**[2,3], and **Kathleen L. Gould**[1]

[1]Howard Hughes Medical Institute and Department of Cell and Developmental Biology, Vanderbilt University School of Medicine, Nashville, TN 37232, US

[2]Department of Biological Sciences, Department of Cell and Developmental Biology, Vanderbilt University, Nashville, TN 37235, US

[3]Department of Developmental Biology, Washington University School of Medicine, St. Louis, MO 63110, US

Abstract

Cyclin-dependent kinases (Cdk) and their counteracting phosphatases are key regulators of cell cycle progression. In yeasts, the Cdc14 family of phosphatases promotes exit from mitosis and progression through cytokinesis by reversing phosphorylation of Cdk1 substrates. In vertebrates, CDC14 paralogs, CDC14A and CDC14B, have so far been implicated in processes ranging from DNA damage repair, meiosis, centrosome duplication to ciliogenesis. However, the question of whether CDC14 paralogs can functionally compensate for each other has yet to be addressed. Here, using antisense morpholino oligonucleotides to inhibit Cdc14A1 function, we observed that Cdc14A1 depleted zebrafish embryos displayed ventrally curved body and left-right asymmetry defects, similarly to Cdc14B deficient embryos and zebrafish mutants with cilia defects. Accordingly, we found that Cdc14A1, like Cdc14B, plays a role in ciliogenesis in the Kupffer's vesicle (KV) and other ciliated tissues, and can do so independently of its function in cell cycle. Furthermore, we observed reciprocal suppression of KV cilia length defects of Cdc14A1 and Cdc14B deficient embryos by *cdc14b* and *cdc14a1* RNAs, respectively. Together, these studies demonstrate for the first time that Cdc14A and Cdc14B have overlapping functions in the ciliogenesis process during zebrafish development.

Keywords

Cell cycle; Ciliogenesis; Left-Right asymmetry; Kupffer's vesicle

INTRODUCTION

Oscillation in the activity of the Cyclin-dependent kinases (Cdks) is a key driver of progression through the cell cycle (Morgan, 1997). By counteracting the activity of the Cdks via dephosphorylation of their substrates, the Cdc14 family of phosphatases facilitates exit from mitosis and the process of cytokinesis, at least in yeasts (Trinkle-Mulcahy and Lamond, 2006; Bouchoux and Uhlmann, 2011; Wurzenberger and Gerlich, 2011).

Cdc14 phosphatases have been conserved throughout evolution. In *Saccharomyces cerevisiae* and *Schizosaccharomyces pombe*, these enzymes accomplish analogous functions during mitosis and cytokinesis (Stegmeier and Amon, 2004; Clifford et al., 2008; Mocciaro

Contact: kathy.gould@vanderbilt.edu, Phone: 615 343 9502, FAX: 615 343 0723.

and Schiebel, 2010). In vertebrates, the situation is more complex since a duplication of the *CDC14* gene occurred. At least two members of the CDC14 family, CDC14A and CDC14B, have been described in human, mouse, chick, *Xenopus laevis* and zebrafish (Li et al., 2000; Kaiser et al., 2004; Krasinska et al., 2007; Mocciaro et al., 2010; Clément et al., 2011). Previous studies have uncovered multiple and, in many cases, divergent functions for each of these enzymes. Indeed, CDC14A was found to play a role in mitotic timing (Vazquez-Novelle et al., 2010; Sacristan et al., 2011), cytokinesis (Bembenek and Yu, 2001; Kaiser et al., 2002; Mailand et al., 2002; Kaiser et al., 2004; Krasinska et al., 2007), meiosis (Schindler and Schultz, 2009b), DNA repair (Mocciaro et al., 2010) and transcriptional repression (Clemente-Blanco et al., 2011), whereas CDC14B was implicated in G1-phase length regulation (Rodier et al., 2008), centriole duplication (Wu et al., 2008), mitosis (Tumurbaatar et al., 2011), spindle stability (Cho et al., 2005), meiosis (Schindler and Schultz, 2009a), DNA damage response (Bassermann et al., 2008; Mocciaro et al., 2010) or repair (Mocciaro et al., 2010; Wei et al., 2011), activation of the zygotic genome (Buffone et al., 2009), ciliogenesis (Clément et al., 2011) and oncogenic transformation (Chiesa et al., 2011).

Possibly accounting for functional differences, CDC14A and CDC14B localize to distinct sub-cellular compartments. Whether endogenous or GFP-fused, CDC14A is observed at the centrosome during interphase (Bembenek and Yu, 2001; Kaiser et al., 2002; Mailand et al., 2002; Kaiser et al., 2004; Krasinska et al., 2007; Schindler and Schultz, 2009b; Mocciaro et al., 2010), and the spindle (Schindler and Schultz, 2009b) and midbody (Krasinska et al., 2007) during mitosis. In contrast, endogenous and tagged CDC14B proteins are detected in the nucleolus during interphase (Kaiser et al., 2002; Mailand et al., 2002; Berdougo et al., 2008; Mocciaro et al., 2010; Clément et al., 2011) as well as the centrosomes (Wu et al., 2008) and microtubules (Cho et al., 2005). During mitosis and meiosis, Cdc14B localizes at the spindle (Buffone et al., 2009; Schindler and Schultz, 2009b; Schindler and Schultz, 2009a; Clément et al., 2011), the spindle poles (Schindler and Schultz, 2009a) and the chromosomes (Berdougo et al., 2008). The reported functional differences and distinct sub-cellular localizations between CDC14A and CDC14B might suggest that these phosphatases evolved towards independent roles. However, human CDC14A and CDC14B can both rescue the reduced size characteristic of Clp1-deficient *S. pombe* strains (Vazquez-Novelle et al., 2005). In addition, both Cdc14A and Cdc14B were separately reported to regulate progression through mitosis via dephosphorylation of Cdc25 (Vazquez-Novelle et al., 2010; Tumurbaatar et al., 2011). Moreover, cells lacking either Cdc14A or Cdc14B are deficient in DNA repair (Mocciaro et al., 2010). Thus, it is currently unclear whether Cdc14A and Cdc14B are functionally overlapping and the possibility that these enzymes are functionally redundant has not been directly tested.

Recently we reported that, in zebrafish, Cdc14B regulates cilia length in various tissues such as the Kupffer's vesicle (KV, the organ of asymmetry in zebrafish, analogous to the node in mouse), the posterior kidney duct and the inner ear (Clément et al., 2011). Because CDC14A localizes at centrosomes during interphase (Bembenek and Yu, 2001; Kaiser et al., 2002; Mailand et al., 2002; Kaiser et al., 2004; Krasinska et al., 2007; Mocciaro et al., 2010), when the cilium is present at the cell surface, but is absent from this structure or present at a low level during mitosis, when the cilium is absent (Dawe et al., 2007; Schindler and Schultz, 2009b), we wondered whether zebrafish. CDC14A, like zebrafish Cdc14B, could also be involved in the process of ciliogenesis.

Using an antisense morpholino oligonucleotide (MO) approach to inhibit Cdc14A1 expression during early zebrafish development, we found that embryos deficient for Cdc14A1 displayed a morphological phenotype similar to that of Cdc14B depleted embryos (Clément et al., 2011) and of zebrafish mutants with cilia defects (Kramer-Zucker et al.,

2005; Bisgrove and Yost, 2006), i.e. curved body and abnormal left-right (LR) asymmetry. Consistent with the LR asymmetry defect, the cilia were shorter in the KV of *cdc14a1* morphant embryos. This result, despite the different sub-cellular localization between Cdc14A1 and Cdc14B, prompted us to investigate the possible functional redundancy between these phosphatases. Reciprocal suppression experiments testing the ability of Cdc14A1 to restore cilia length in the KV of Cdc14B depleted embryos, and vice versa, indicate that Cdc14A1 and Cdc14B are partially redundant for their role in ciliogenesis in the KV. This first evidence for a redundant function between two members of the Cdc14 family raises the possibility that eliminating the function of two or more paralogs of CDC14 might be necessary to uncover the full range of CDC14 functions in vertebrates.

RESULTS

Cdc14A1 expression pattern and sub-cellular localization

We previously reported that three *cdc14* paralogs could be discerned in the zebrafish genome, one encoding a Cdc14B enzyme and two, *cdc14a1* and *cdc14a2*, encoding Cdc14A enzymes. Using a 24 hours post-fertilization (hpf) cDNA library, we identified two isoforms of *cdc14a1*, *cdc14a1_tv1* and *cdc14a1_tv2* (Clément et al., 2011), although others might exist. These two transcript variants differ by the absence of exon 14 in the sequence of *cdc14a1_tv2* (Fig. 1A). Whole-mount in situ hybridization and RT-PCR experiments indicated that *cdc14a1* transcripts encoding both isoforms were maternally provided and expressed ubiquitously throughout embryogenesis and early larval development (Supp. Fig. S1).

Cdc14A has previously been reported to accumulate at centrosomes during interphase in *X. laevis*, chick and human cells (Bembenek and Yu, 2001; Kaiser et al., 2002; Mailand et al., 2002; Kaiser et al., 2004; Krasinska et al., 2007; Mocciaro et al., 2010). Due to the lack of antibody, we assayed Cdc14A1 sub-cellular localization by over-expressing *cdc14a1*. Synthetic *cdc14a1_tv1-GFP* RNA was first injected in embryos at the one-cell stage and its expression was then monitored in vivo in the ectoderm at 8 hpf. We observed that Cdc14A1-GFP co-localized with centrin, a centriole marker (Fig. 1B, yellow arrowheads). This suggested that as in other species, zebrafish Cdc14A1 localized to centrosomes during interphase. Moreover, following the localization of Cdc14A1-GFP in dividing cells, we found that, in accordance with the localization of CDC14A enzymes in other organisms (Schindler and Schultz, 2009b), Cdc14A1 was also present at the spindle poles (Fig. 1C, yellow arrowheads) and the spindle (red asterisk) during mitosis. Further analysis in ciliated cells from the ectoderm of 14 hpf embryos fixed and stained for GFP, acetylated-tubulin and γ-tubulin (another marker of the centriole) in order to enhance the signals, revealed that Cdc14A1-GFP partially co-localized with γ-tubulin, (Fig. 1D, yellow arrowheads). However, its expression did not overlap with acetylated-tubulin that marks the cilium (between blue arrows). This suggested that Cdc14A1 phosphatase was present at the base of the cilium, possibly in part at the basal body. Interestingly, Cdc14 has recently been found to also localize at the basal body in *Phytophthora infestans* (Ah-Fong and Judelson, 2011).

Morphological characterization of Cdc14A1 loss of function

To understand the role of Cdc14A1 during zebrafish embryogenesis, we used two MOs that were designed to target both characterized isoforms of *cdc14a1* by interfering either with splicing (MO1-*cdc14a1*) or with translation (MO2-*cdc14a1*) (Fig. 2A, purple bars). For each MO, different doses were tested in order to establish the threshold at which the MOs were efficiently producing a phenotype. No evident morphological phenotype was detected following the injection at the one-cell stage of 4 ng of MO1-*cdc14a1* (Fig. 2D,M), 1 ng of MO2-*cdc14a1* or H_2O alone. When embryos were injected with 5 or 6 ng of MO1-*cdc14a1*

or 3.5 ng of MO2-*cdc14a1*, some of them displayed a curved body shape with respect to the dorsal-ventral axis at 31 hpf and 3 dpf, when compared to wild-type embryos. However, this phenotype was consistently observed when the embryos were injected with 8 ng of MO1-*cdc14a1* and 4.5 ng of MO2-*cdc14a1* at 31 hpf (Fig. 2C,E,F) and 3 dpf (Fig. 2L,N,O). These latter doses were used for our experiments.

Since body curvature can result from the injection procedure itself, we injected embryos with H_2O to rule out this possibility. We found that the curved body shape was not due to the injection per se (Supp. Fig. S2A–C). In addition, by injecting *cdc14a1* synthetic RNA into MO1-*cdc14a1* injected embryos, we could partially rescue this morphological phenotype (Supp. Fig. S2D,E), suggesting that the curved body phenotype is specifically due to the effect of Cdc14A1 loss of function. The incomplete rescue may be due to the existence of additional *cdc14a1* transcript variants also affected by the MOs and we note that we detected several differentially spliced transcripts of each *cdc14* gene we have examined (Clément et al., 2011).

The efficiency of 8 ng of MO1-*cdc14a1* was measured by RT-PCR over time (Fig. 2B). At 10 hpf, no wild-type transcripts were detected, but a weak wild-type transcript was detected again at 24 hpf. Sequence analysis revealed the insertion of intron 2 in one type of aberrant isoform (Fig. 2A,B, red asterisk) and the loss of exon 2 in the second type of aberrant transcript (Fig. 2A,B, blue asterisk). Both changes led to frame shifts and subsequently premature stop codons early in the sequence. Therefore, the resulting truncated proteins were likely to be non functional.

Cdc14A1 depleted embryos exhibited a milder morphological phenotype compared to *cdc14b* morphant embryos (Fig. 2G,P) (Clément et al., 2011) and other mutants with cilia defects (Cantagrel et al., 2008; Wessely and Obara, 2008; Li and Sun, 2011; Zhao et al., 2012). Indeed, hydrocephaly and kidney cysts were only rarely observed when Cdc14A1 function was reduced. In addition, the reduction in the body size of the Cdc14A1 deficient embryos was also less pronounced than in *cdc14b* morphant embryos (compare panels D–F to G in Fig. 2). This relatively mild nature of the *cdc14a1* phenotype could be due to incomplete loss of Cdc14A1 function or functional redundancy with Cdc14A2, encoded by the other zebrafish *cdc14a* gene (Clément et al., 2011), among other possibilities.

Role of Cdc14A1 in LR asymmetry establishment

Despite the mild morphological phenotype of *cdc14a1* morphants in comparison to that of *cdc14b*, we wanted to know if there were further similarities between the *cdc14a1* and *cdc14b* phenotypes. Given the LR asymmetry defects previously reported for Cdc14B depleted embryos (Clément et al., 2011), we investigated if *cdc14a1* morphant embryos also displayed such a phenotype. Using *nkx2.5* as a heart marker (Chen and Fishman, 1996) at 31 hpf, we observed that the heart tube was left-shifted in the majority of wild-type embryos (Fig. 3A), but that its shifting in *cdc14a1* and *cdc14b* morphant embryos (Fig. 3B,C) was randomized (Fig. 3D) (Clément et al., 2011). Indeed, while in 97% of wild-type embryos the heart tube was oriented to the left, only 50 to 60% of *cdc14* morphant embryos showed this left-orientation. Similarly, our analyses of *foxa3* (Odenthal and Nusslein-Volhard, 1998) expression at 50 hpf revealed that the location of the visceral organs and the gut looping were randomized in Cdc14A1 and Cdc14B deficient embryos (Fig. 3F,G) when compared to wild-type control embryos (Fig. 3E). Whereas 93% of wild-type control embryos presented a left-directed gut looping, no more than 35 to 47% of *cdc14a1* and *cdc14b* morphant embryos exhibited this phenotype (Fig. 3H). Further, the expression of *southpaw* (*spaw*), an early marker of asymmetry (Long et al., 2003), in the lateral plate mesoderm at 18 hpf was also affected in *cdc14a1* and *cdc14b* morphants (Fig. 3J,K) in comparison to wild-type embryos (Fig. 3I). *spaw* expressed in the left lateral plate mesoderm in 93% of wild-type

control embryos compared to only 25 to 31% of Cdc14A1 and Cdc14B depleted embryos (Fig. 3L). Interestingly, while in *cdc14a1* morphant embryos *spaw* is mostly not expressed, Cdc14B deficient embryos rather display an expression in the right lateral plate mesoderm. One explanation is that all KV cells did not receive a similar dose of MOs. Thus, some cells could present short cilia while some others would display cilia of correct length. Depending on how these cells are distributed within the KV, the fluid flow and consequently *spaw* expression could be differently affected. In addition, we found previously that most *cdc14b* morphants displayed an absence of *spaw* expression (Clément et al., 2011), which is in accord with this hypothesis.

Thus, we found that similarly to Cdc14B deficient embryos, depletion of Cdc14A1 led to defects in the specification of LR asymmetry.

Cdc14A1 has a role in ciliogenesis

Specification of LR asymmetry begins in the organ of asymmetry, the KV, located at the posterior end of the embryo (Essner et al., 2005). Within the KV, cilia beating in a counter clockwise manner is thought to produce a directional fluid flow that triggers a cascade of events culminating in the expression of markers on the left or right side of the embryo and later, asymmetric placement and morphology of the organs (Essner et al., 2005). Thus, the LR asymmetry defects observed in the *cdc14a1* morphant embryos prompted us to investigate its effect on ciliogenesis in the KV. To this end, we injected embryos at the one-cell stage with MO1-*cdc14a1* or at 3 hpf, when the yolk syncytial layer has separated from the embryo proper (Kimmel and Law, 1985), with MO1- or MO2-*cdc14a1*. By injecting into the yolk syncytial layer at this later stage of development, we aimed to specifically target the dorsal forerunner cells (DFCs) that will form the KV (Cooper and D'Amico, 1996; Melby et al., 1996). The embryos were then stained at 14 hpf using an antibody against acetylated-tubulin to mark the cilia. Upon acquisition of Z-stacks and reconstruction of the whole KV, we counted the number of cilia in the KV and measured their length. The number of KV cilia and KV cells was similar between non-injected control embryos and *cdc14a1* MO-injected embryos, except when MO1-*cdc14a1* was injected at 3 hpf. In that case, the number of KV cilia was decreased by 31.5 % (Fig. 4A–C) and injection of the *cdc14a1* MOs in *Tg[sox17:GFP]* embryos, in which KV cells are GFP-labelled, showed that the number of KV cells was significantly reduced when MO1-*cdc14a1* was injected at 3 hpf (Fig. 4D).

Interestingly however, the length of KV cilia was significantly reduced in all Cdc14A1 depleted embryos (Fig. 4B) when compared to non-injected control wild-type embryos (Fig. 4A), independently of the *cdc14a1* MO used and the time of injection (Fig. 4E). Because injection of *cdc14a1* MOs at 3 hpf led to shorter cilia, this supports the notion that Cdc14A1 specifically acts in the KV ciliated cells. However, a reduction of only 12% in cilia length was observed when MO1-*cdc14a1* was injected at the one-cell stage, whereas a more significant reduction of 32 and 48% was seen when MO1-*cdc14a1* or MO2-*cdc14a1* were injected at 3 hpf, respectively. It is interesting to note that the reduction of the length of cilia was greater when *cdc14a1* MOs were injected at 3 hpf rather than at the one-cell stage. This could be due to a dose effect of the MOs, since optimal doses for both types of injection were the same while the number of targeted cells differed between the two techniques. Another possibility is that due to Cdc14A1 function in cell cycle control, KV cell division, which occurs between 8 and 10 hpf (Cooper and D'Amico, 1996; Amack et al., 2007), could have been delayed. As a consequence, KV would be smaller and KV cilia would not be able to grow to the expected length. However, when comparing the injection of MO1- and MO2-*cdc14a1* at 3 hpf, we found that despite a smaller number of KV cells in MO1-*cdc14a1* injected embryos, KV cilia were longer than those in MO2-*cdc14a1* injected embryos (Fig. 4D,E). Thus, the decrease of KV cilia length cannot solely be due to Cdc14A1 function in cell cycle control.

To verify that the reduction in KV cilia length in Cdc14A1 depleted embryos resulted specifically from Cdc14A1 loss of function, we used a rescue strategy in which MO1-*cdc14a1* and synthetic *cdc14a1_tv1* and *cdc14a1_tv2* RNAs were sequentially injected. Importantly, these synthetic RNAs did not possess a binding site for MO1-*cdc14a1* and therefore the rescue does not occur by titration of the MO. MO1-*cdc14a1* was injected at the one-cell stage and *cdc14a1* RNAs were injected at 3 hpf. As a result, RNAs injected in the yolk at this stage of development specifically targeted DFCs and thus the future KV ciliated cells. The same method of cilia measurement as described above was used to assay the rescue at 14 hpf. We found that the shortened KV cilia length in *cdc14a1* morphant embryos could partially be suppressed upon injection of *cdc14a1* RNAs (Fig. 4E). In addition, using these techniques of injections, we could also partially rescue the LR asymmetry defect of the MO1-*cdc14a* injected embryos (Fig. 3M). Whereas the heart tube was shifted to the left in 47 % of Cdc14A1 depleted embryos, a significant 64 % of *cdc14a1* morphant embryos showed a left-shifting after injection of *cdc14a1* RNAs at 3 hpf. Taken together, these data indicate that, similar to Cdc14B, Cdc14A1 plays a role in ciliogenesis in the KV.

The effect of Cdc14A1 loss of function on ciliogenesis was not restricted to the KV. The length of motile cilia in the posterior kidney duct was also reduced in MO2-*cdc14a1* injected embryos when compared to non-injected control embryos (Suppl. Fig. S3A). However, we did not observe such phenotype when MO1-*cdc14a1* was injected. This could be explained by the presence of other transcript variants of *cdc14a1*. The length of the primary cilia in the posterior macula of the inner ear were also affected when *cdc14a1* MOs were injected (Suppl. Fig. S3B).

Functional redundancy between Cdc14A1 and Cdc14B

Despite the different sub-cellular localizations of CDC14A and CDC14B, these enzymes are nonetheless found to function in common processes. This raises the possibility that in some cases, CDC14 paralogs may compensate for each other's function. To test this hypothesis, we used the *cdc14b*^{vu426} hypomorphic insertional mutant allele to carry double loss of function experiments. Although homozygous *cdc14b*$^{vu426/vu426}$ mutants show a decrease in the expression of *cdc14b* transcripts, they do not exhibit any morphological phenotypes or LR asymmetry defects (Clément et al., 2011) (Fig. 2H,Q and Fig. 5A). This is possibly due in part to compensatory activity of Cdc14A1 and/or Cdc14A2. To test this possibility, we injected low doses of MO1-*cdc14a1* into *cdc14b*$^{vu426/vu426}$ homozygous mutant embryos. Injection of 4 ng of MO1-*cdc14a1* in wild-type embryos at the one-cell stage had not given rise to an overt morphological phenotype (Fig. 2D,M). However, *cdc14b*$^{vu426/vu426}$ mutants injected with the same dose of MO1-*cdc14a1* presented with a curved body (Fig. 2I,R), as seen with injection of higher doses of MO1-*cdc14a1* in wild-type embryos (Fig. 2E,N). In addition to the morphological phenotype, we also assayed LR asymmetry defects by looking at the orientation of the heart tube shift at 31 hpf. Whereas injection of 4 ng of MO1-*cdc14a1* in wild-type embryos led to a weak LR asymmetry phenotype (92% of embryos with a left-shifted heart tube compared to 99% in wild-type embryos), *cdc14b*$^{vu426/vu426}$ mutant embryos injected with the same dose of MO displayed a significantly higher penetrance of the randomized heart tube shifting (71% of embryos with a heart tube shifting to the left) (Fig. 5A). Finally, we measured the length of KV cilia in embryos injected at the one cell stage with sub-threshold of MO1-*cdc14a1* and MO1-*cdc14b*. KV cilia were significantly shorter when both *cdc14* genes were targeted in comparison to KV cilia from non-injected control embryos or embryos injected with sub-threshold of one MO (Fig. 5B). Because injection of 8 ng of MO1-*cdc14a1* in a wild-type background conferred a phenotype similar to the one caused by injection of a sub-threshold of MO1-*cdc14a1* in a sensitized background, this further corroborated the specificity of MO1-*cdc14a1* previously shown by the similarity in the phenotype of embryos injected with either one of the *cdc14a1*

MOs (Fig. 2E,F,N,O) and by the rescue of the KV cilia length in *cdc14a1* morphant embryos (Fig. 4E).

Because our results indicated that both Cdc14A1 and Cdc14B play a role in ciliogenesis in the KV, we decided to address the possibility that these two Cdc14 phosphatases were functionally redundant in this process. Specifically, we asked whether loss of Cdc14A1 function could be compensated by overexpression of *cdc14b* RNA and reciprocally if loss of Cdc14B function could be balanced by *cdc14a1* overexpression. We therefore performed a series of experiments in which embryos deficient for Cdc14A1 were injected at 3 hpf with synthetic *cdc14a1* or *cdc14b* RNAs, and conversely, in which embryos depleted for Cdc14B were injected at 3 hpf with *cdc14b* or *cdc14a1* RNAs. To assay the degree of phenotypic suppression, we stained 14 hpf embryos with an anti-acetylated tubulin antibody and we measured the length of the cilia in the KV as described above. We found that the shortening of the KV cilia length of *cdc14a1* morphant embryos could be suppressed by the injection of *cdc14a1* or *cdc14b* RNAs (Fig. 6A). Taking advantage of the variation in the length of the KV cilia throughout the organ, we examined the reciprocal suppression experiment in greater detail and determined the length distribution of the KV cilia. We found that cilia length in the KV of Cdc14A1 depleted embryos (Fig. 6B, red) could be almost equally increased whether *cdc14a1* or *cdc14b* RNAs were injected (Fig. 6B, compare yellow and pink columns). Likewise, cilia length in the KV of *cdc14b* deficient embryos could be increased after injection of either *cdc14b* or *cdc14a1* RNAs (Fig. 6A). As for Cdc14A1 deficient embryos, analysis of cilia length distribution in the KV of Cdc14B depleted embryos (Fig. 6C, red) revealed that cilia length was also almost equally augmented whether *cdc14a1* or *cdc14b* RNAs were injected (Fig. 6C, compare yellow and pink columns). Altogether, our data indicate that in zebrafish, Cdc14A1 and Cdc14B phosphatases compensate for each other function in the process of KV ciliogenesis.

DISCUSSION

Here, we analyzed the function of Cdc14A1 during zebrafish embryonic development. Using two different antisense MOs to inhibit Cdc14A1 function, we found that, similar to Cdc14B, Cdc14A1 plays a role in the process of ciliogenesis in the KV, and can do so independently of its function in cell cycle control. Furthermore, via a series of phenotype suppression experiments, we provide evidence that Cdc14A1 and Cdc14B can functionally compensate for each other in the process of ciliogenesis in the KV.

Consistent with previous studies in human, chicken and Xenopus cells (Bembenek and Yu, 2001; Kaiser et al., 2002; Mailand et al., 2002; Kaiser et al., 2004; Krasinska et al., 2007; Mocciaro et al., 2010), we found that zebrafish Cdc14A1 is present at the centrosomes during interphase. Further study in ciliated ectodermal cells of 14 hpf embryos revealed that Cdc14A1 is also present at the base of the cilium and possibly at the basal body from which the cilium emanates. This is the first report of this localization for Cdc14 enzymes. In contrast with Cdc14A1, zebrafish Cdc14B is not detected at the centrosomes (Clément et al., 2011). However, despite their distinct sub-cellular localization, the functional redundancy between these two Cdc14 family members suggests that they share the same or at least overlapping substrates. Regulation of ciliogenesis via phosphorylation and dephosphorylation is not uncommon. Kinases and phosphatases are anchored in the ciliary axoneme and have previously been reported to regulate cilia motility (Wirschell et al., 2011) as well as cilia stability (Wang and Brautigan, 2008). In addition, phosphoregulation of ciliogenesis from the basal body has also been described. Indeed, Aurora A phosphorylates and activates HDAC6, a tubulin deacetylase, thus promoting destabilization and disassembly of the cilium (Pugacheva et al., 2007). The identification of Cdc14 substrates now becomes an important next step if we want to dissect further their mechanism of action in the process

of ciliogenesis. This is all the more interesting considering the role of Cdc14 enzymes in cell cycle progression and the fact that ciliogenesis is a cell cycle regulated process.

Though compensating for each other in the KV, a difference between Cdc14A1 and Cdc14B is the severity of the overall morphological phenotype caused by loss of function of each enzyme. For example, kidney cysts and hydrocephaly, characteristics often associated with defects in ciliogenesis in zebrafish (Wessely and Obara, 2008), were frequently observed in *cdc14b* depleted embryos (Clément et al., 2011), whereas these events occurred only rarely in *cdc14a1* morphant embryos. One explanation would be that, unlike Cdc14B, Cdc14A1 does not function in ciliogenesis in tissues other than the KV. It is also possible that Cdc14A2 compensates for its ciliogenesis function in other tissues.

In conclusion, our study focusing on the process of ciliogenesis in the KV has revealed for the first time functional redundancy between Cdc14A and Cdc14B enzymes. While the possibility of overlapping function between these paralogs has been raised previously by the finding that mammalian Cdc14A and Cdc14B function in common pathways such as DNA repair and dephosphorylation of Cdc25 during mitosis (Mocciaro et al., 2010; Vazquez-Novelle et al., 2010; Tumurbaatar et al., 2011), genetic evidence supporting this possibility has not previously been reported in any other vertebrate organism. In light of our data, it becomes likely that a more global functional redundancy is to be expected between CDC14 paralogs.

EXPERIMENTAL PROCEDURES

Zebrafish maintenance and staging

Wild-type AB*, *cdc14b*$^{vu426/vu426}$ and *Tg[sox17:GFP]* (Sakaguchi et al., 2006) adult zebrafish, *Danio rerio*, were maintained as previously described (Solnica-Krezel et al., 1996). Embryos/larvae were staged according to morphology (Kimmel et al., 1995).

Morpholino and mRNA injections

Two antisense MOs (Gene tools, LLC, Philomath, OR, US) were designed to target *cdc14a1* isoforms: MO1-*cdc14a1* (MORPH1732, 5'-TTTAGTTTGGGCAGACTCACTTTTC-3') and MO2-*cdc14a1* (MORPH1731, 5'-CAGCTCACTGTCTCCCATTTTATTC-3'). MO1-*cdc14b*, targeting *cdc14b* isoforms, has been previously described (Clément et al., 2011).

Microinjections were done using a PV820 picopump (World Precision Instrument, Sarasota, FL, US) which possesses a hold pressure function to eliminate the risk of fluid uptake by the injection needle and therefore prevent from fluctuation in the amount of MOs injected. A micrometer was also used to measure the volume of MO injected every 30 embryos.

For the rescue and protein localization, synthetic mRNAs from *cdc14a1_tv1*, *cdc14a1_tv2* (GFP tagged or not), *cdc14b_tv1* and *mcherry-centrin* (gift from Adrian Salic) were made by in vitro transcription using the mMessage mMachine System kit (Ambion, Austin, TX, US).

Whole mount in situ hybridization and immunohistochemistry

Embryos and larvae were fixed in 4% paraformaldehyde overnight and then permeabilized with Proteinase K (10 μg/ml, Roche, Mannheim, Germany). For in situ hybridization, embryos and larvae were hybridized overnight at 68°C with the following digoxigenin labelled probes: *cdc14a1_tv1*, *cdc14a1_tv2*, *nkx2.5* (Chen and Fishman, 1996), *foxa3* (Odenthal and Nusslein-Volhard, 1998) and *southpaw* (Long et al., 2003). Detection and staining were done as previously described (Thisse and Thisse, 2008). For

immunohistochemistry, embryos were incubated with the following primary antibodies: rabbit anti-GFP (1:500, Torrey Pines Biolabs Inc, East Orange, NJ, US), mouse anti-acetylated tubulin (1:250, Sigma-Aldrich Corp., St. Louis, MO, US) and mouse anti-γ-tubulin (1:500, Sigma-Aldrich Corp., St. Louis, MO, US). Secondary antibodies were goat anti-rabbit or anti-mouse (Invitrogen, Carlsbad, CA, US). Nuclei were counterstained with TOPRO-3 (Molecular Probes, Inc., Eugene, OR, US).

Imaging

Images were acquired using an Imager Z1 compound microscope and AxioVision software (Zeiss, Oberkochen, Germany) for the embryos stained by in situ hybridization and with an LSM510 inverted confocal microscope (Zeiss, Oberkochen, Germany) and the LSM Image acquisition software (Version 4.2.0.121, Zeiss, Oberkochen, Germany) for in vivo experiments and for the embryos stained by immunohistochemistry.

Supplementary Material

Refer to Web version on PubMed Central for supplementary material.

Acknowledgments

The authors thank members of the Gould and Solnica-Krezel labs for many valuable discussions and comments on the manuscript, Dr. B. Blanco-Sanchez for his help with imaging and SC Zebrafish Facility staff for excellent fish care. This work was supported by a Martha Rivers Ingram endowment to LSK and the HHMI, of which KLG is an investigator.

REFERENCES

Ah-Fong AM, Judelson HS. New role for Cdc14 phosphatase: localization to basal bodies in the oomycete phytophthora and its evolutionary coinheritance with eukaryotic flagella. PLoS One. 2011; 6:e16725. [PubMed: 21340037]

Amack JD, Wang X, Yost HJ. Two T-box genes play independent and cooperative roles to regulate morphogenesis of ciliated Kupffer's vesicle in zebrafish. Dev Biol. 2007; 310:196–210. [PubMed: 17765888]

Bassermann F, Frescas D, Guardavaccaro D, Busino L, Peschiaroli A, Pagano M. The Cdc14B-Cdh1-Plk1 axis controls the G2 DNA-damage-response checkpoint. Cell. 2008; 134:256–267. [PubMed: 18662541]

Bembenek J, Yu H. Regulation of the anaphase-promoting complex by the dual specificity phosphatase human Cdc14a. J Biol Chem. 2001; 276:48237–48242. [PubMed: 11598127]

Berdougo E, Nachury MV, Jackson PK, Jallepalli PV. The nucleolar phosphatase Cdc14B is dispensable for chromosome segregation and mitotic exit in human cells. Cell Cycle. 2008; 7:1184–1190. [PubMed: 18418058]

Bisgrove BW, Yost HJ. The roles of cilia in developmental disorders and disease. Development. 2006; 133:4131–4143. [PubMed: 17021045]

Bouchoux C, Uhlmann F. A quantitative model for ordered Cdk substrate dephosphorylation during mitotic exit. Cell. 2011; 147:803–814. [PubMed: 22078879]

Buffone MG, Schindler K, Schultz RM. Overexpression of CDC14B causes mitotic arrest and inhibits zygotic genome activation in mouse preimplantation embryos. Cell Cycle. 2009; 8:3904–3913. [PubMed: 19923902]

Cantagrel V, Silhavy JL, Bielas SL, Swistun D, Marsh SE, Bertrand JY, Audollent S, Attie-Bitach T, Holden KR, Dobyns WB, Traver D, Al-Gazali L, Ali BR, Lindner TH, Caspary T, Otto EA, Hildebrandt F, Glass IA, Logan CV, Johnson CA, Bennett C, Brancati F, Valente EM, Woods CG, Gleeson JG. Mutations in the cilia gene ARL13B lead to the classical form of Joubert syndrome. Am J Hum Genet. 2008; 83:170–179. [PubMed: 18674751]

Chen JN, Fishman MC. Zebrafish tinman homolog demarcates the heart field and initiates myocardial differentiation. Development. 1996; 122:3809–3816. [PubMed: 9012502]

Chiesa M, Guillamot M, Bueno MJ, Malumbres M. The Cdc14B phosphatase displays oncogenic activity mediated by the Ras-Mek signaling pathway. Cell Cycle. 2011; 10:1607–1617. [PubMed: 21502810]

Cho HP, Liu Y, Gomez M, Dunlap J, Tyers M, Wang Y. The dual-specificity phosphatase CDC14B bundles and stabilizes microtubules. Mol Cell Biol. 2005; 25:4541–4551. [PubMed: 15899858]

Clément A, Solnica-Krezel L, Gould KL. The Cdc14B phosphatase contributes to ciliogenesis in zebrafish. Development. 2011; 138:291–302. [PubMed: 21177342]

Clemente-Blanco A, Sen N, Mayan-Santos M, Sacristan MP, Graham B, Jarmuz A, Giess A, Webb E, Game L, Eick D, Bueno A, Merkenschlager M, Aragon L. Cdc14 phosphatase promotes segregation of telomeres through repression of RNA polymerase II transcription. Nat Cell Biol. 2011

Clifford DM, Chen CT, Roberts RH, Feoktistova A, Wolfe BA, Chen JS, McCollum D, Gould KL. The role of Cdc14 phosphatases in the control of cell division. Biochem Soc Trans. 2008; 36:436–438. [PubMed: 18481975]

Cooper MS, D'Amico LA. A cluster of noninvoluting endocytic cells at the margin of the zebrafish blastoderm marks the site of embryonic shield formation. Dev Biol. 1996; 180:184–198. [PubMed: 8948584]

Dawe HR, Farr H, Gull K. Centriole/basal body morphogenesis and migration during ciliogenesis in animal cells. J Cell Sci. 2007; 120:7–15. [PubMed: 17182899]

Essner JJ, Amack JD, Nyholm MK, Harris EB, Yost HJ. Kupffer's vesicle is a ciliated organ of asymmetry in the zebrafish embryo that initiates left-right development of the brain, heart and gut. Development. 2005; 132:1247–1260. [PubMed: 15716348]

Kaiser BK, Nachury MV, Gardner BE, Jackson PK. Xenopus Cdc14 alpha/beta are localized to the nucleolus and centrosome and are required for embryonic cell division. BMC Cell Biol. 2004; 5:27. [PubMed: 15251038]

Kaiser BK, Zimmerman ZA, Charbonneau H, Jackson PK. Disruption of centrosome structure, chromosome segregation, and cytokinesis by misexpression of human Cdc14A phosphatase. Mol Biol Cell. 2002; 13:2289–2300. [PubMed: 12134069]

Kimmel CB, Ballard WW, Kimmel SR, Ullmann B, Schilling TF. Stages of embryonic development of the zebrafish. Dev Dyn. 1995; 203:253–310. [PubMed: 8589427]

Kimmel CB, Law RD. Cell lineage of zebrafish blastomeres. II. Formation of the yolk syncytial layer. Dev Biol. 1985; 108:86–93. [PubMed: 3972183]

Kramer-Zucker AG, Olale F, Haycraft CJ, Yoder BK, Schier AF, Drummond IA. Cilia-driven fluid flow in the zebrafish pronephros, brain and Kupffer's vesicle is required for normal organogenesis. Development. 2005; 132:1907–1921. [PubMed: 15790966]

Krasinska L, de Bettignies G, Fisher D, Abrieu A, Fesquet D, Morin N. Regulation of multiple cell cycle events by Cdc14 homologues in vertebrates. Exp Cell Res. 2007; 313:1225–1239. [PubMed: 17292885]

Li J, Sun Z. Qilin is essential for cilia assembly and normal kidney development in zebrafish. PLoS One. 2011; 6:e27365. [PubMed: 22102889]

Li L, Ljungman M, Dixon JE. The human Cdc14 phosphatases interact with and dephosphorylate the tumor suppressor protein p53. J Biol Chem. 2000; 275:2410–2414. [PubMed: 10644693]

Long S, Ahmad N, Rebagliati M. The zebrafish nodal-related gene southpaw is required for visceral and diencephalic left-right asymmetry. Development. 2003; 130:2303–2316. [PubMed: 12702646]

Mailand N, Lukas C, Kaiser BK, Jackson PK, Bartek J, Lukas J. Deregulated human Cdc14A phosphatase disrupts centrosome separation and chromosome segregation. Nat Cell Biol. 2002; 4:317–322. [PubMed: 11901424]

Melby AE, Warga RM, Kimmel CB. Specification of cell fates at the dorsal margin of the zebrafish gastrula. Development. 1996; 122:2225–2237. [PubMed: 8681803]

Mocciaro A, Berdougo E, Zeng K, Black E, Vagnarelli P, Earnshaw W, Gillespie D, Jallepalli P, Schiebel E. Vertebrate cells genetically deficient for Cdc14A or Cdc14B retain DNA damage

checkpoint proficiency but are impaired in DNA repair. J Cell Biol. 2010; 189:631–639. [PubMed: 20479464]

Mocciaro A, Schiebel E. Cdc14: a highly conserved family of phosphatases with non-conserved functions? J Cell Sci. 2010; 123:2867–2876. [PubMed: 20720150]

Morgan DO. Cyclin-dependent kinases: engines, clocks, and microprocessors. Annu Rev Cell Dev Biol. 1997; 13:261–291. [PubMed: 9442875]

Odenthal J, Nusslein-Volhard C. fork head domain genes in zebrafish. Dev Genes Evol. 1998; 208:245–258. [PubMed: 9683740]

Pugacheva EN, Jablonski SA, Hartman TR, Henske EP, Golemis EA. HEF1-dependent Aurora A activation induces disassembly of the primary cilium. Cell. 2007; 129:1351–1363. [PubMed: 17604723]

Rodier G, Coulombe P, Tanguay PL, Boutonnet C, Meloche S. Phosphorylation of Skp2 regulated by CDK2 and Cdc14B protects it from degradation by APC(Cdh1) in G1 phase. EMBO J. 2008; 27:679–691. [PubMed: 18239684]

Sacristan MP, Ovejero S, Bueno A. Human Cdc14A becomes a cell cycle gene in controlling Cdk1 activity at the G/M transition. Cell Cycle. 2011; 10:387–391. [PubMed: 21233601]

Sakaguchi T, Kikuchi Y, Kuroiwa A, Takeda H, Stainier DY. The yolk syncytial layer regulates myocardial migration by influencing extracellular matrix assembly in zebrafish. Development. 2006; 133:4063–4072. [PubMed: 17008449]

Schindler K, Schultz RM. CDC14B acts through FZR1 (CDH1) to prevent meiotic maturation of mouse oocytes. Biol Reprod. 2009a; 80:795–803. [PubMed: 19129509]

Schindler K, Schultz RM. The CDC14A phosphatase regulates oocyte maturation in mouse. Cell Cycle. 2009b; 8:1090–1098. [PubMed: 19270517]

Solnica-Krezel L, Stemple DL, Mountcastle-Shah E, Rangini Z, Neuhauss SC, Malicki J, Schier AF, Stainier DY, Zwartkruis F, Abdelilah S, Driever W. Mutations affecting cell fates and cellular rearrangements during gastrulation in zebrafish. Development. 1996; 123:67–80. [PubMed: 9007230]

Stegmeier F, Amon A. Closing mitosis: the functions of the Cdc14 phosphatase and its regulation. Annu Rev Genet. 2004; 38:203–232. [PubMed: 15568976]

Thisse C, Thisse B. High-resolution in situ hybridization to whole-mount zebrafish embryos. Nat Protoc. 2008; 3:59–69. [PubMed: 18193022]

Trinkle-Mulcahy L, Lamond AI. Mitotic phosphatases: no longer silent partners. Curr Opin Cell Biol. 2006; 18:623–631. [PubMed: 17030123]

Tumurbaatar I, Cizmecioglu O, Hoffmann I, Grummt I, Voit R. Human Cdc14B Promotes Progression through Mitosis by Dephosphorylating Cdc25 and Regulating Cdk1/Cyclin B Activity. PLoS One. 2011; 6:e14711. [PubMed: 21379580]

Vazquez-Novelle MD, Esteban V, Bueno A, Sacristan MP. Functional homology among human and fission yeast Cdc14 phosphatases. J Biol Chem. 2005; 280:29144–29150. [PubMed: 15911625]

Vazquez-Novelle MD, Mailand N, Ovejero S, Bueno A, Sacristan MP. Human Cdc14A phosphatase modulates the G2/M transition through Cdc25A and Cdc25B. J Biol Chem. 2010; 285:40544–40553. [PubMed: 20956543]

Wang W, Brautigan DL. Phosphatase inhibitor 2 promotes acetylation of tubulin in the primary cilium of human retinal epithelial cells. BMC Cell Biol. 2008; 9:62. [PubMed: 19036150]

Wei Z, Peddibhotla S, Lin H, Fang X, Li M, Rosen JM, Zhang P. Early-onset aging and defective DNA damage response in cdc14b-deficient mice. Mol Cell Biol. 2011; 31:1470–1477. [PubMed: 21262768]

Wessely O, Obara T. Fish and frogs: models for vertebrate cilia signaling. Front Biosci. 2008; 13:1866–1880. [PubMed: 17981674]

Wirschell M, Yamamoto R, Alford L, Gokhale A, Gaillard A, Sale WS. Regulation of ciliary motility: conserved protein kinases and phosphatases are targeted and anchored in the ciliary axoneme. Arch Biochem Biophys. 2011; 510:93–100. [PubMed: 21513695]

Wu J, Cho HP, Rhee DB, Johnson DK, Dunlap J, Liu Y, Wang Y. Cdc14B depletion leads to centriole amplification, and its overexpression prevents unscheduled centriole duplication. J Cell Biol. 2008; 181:475–483. [PubMed: 18458157]

Wurzenberger C, Gerlich DW. Phosphatases: providing safe passage through mitotic exit. Nat Rev Mol Cell Biol. 2011; 12:469–482. [PubMed: 21750572]

Zhao C, Omori Y, Brodowska K, Kovach P, Malicki J. Kinesin-2 family in vertebrate ciliogenesis. Proc Natl Acad Sci U S A. 2012; 109:2388–2393. [PubMed: 22308397]

Key findings

- Cdc14A1 is present at the base of the cilium.
- Ciliogenesis in the Kupffer's vesicle is affected in *cdc14a1* depleted embryos.
- Cdc14A1 and Cdc14B phosphatases are functionally redundant in the process of ciliogenesis.

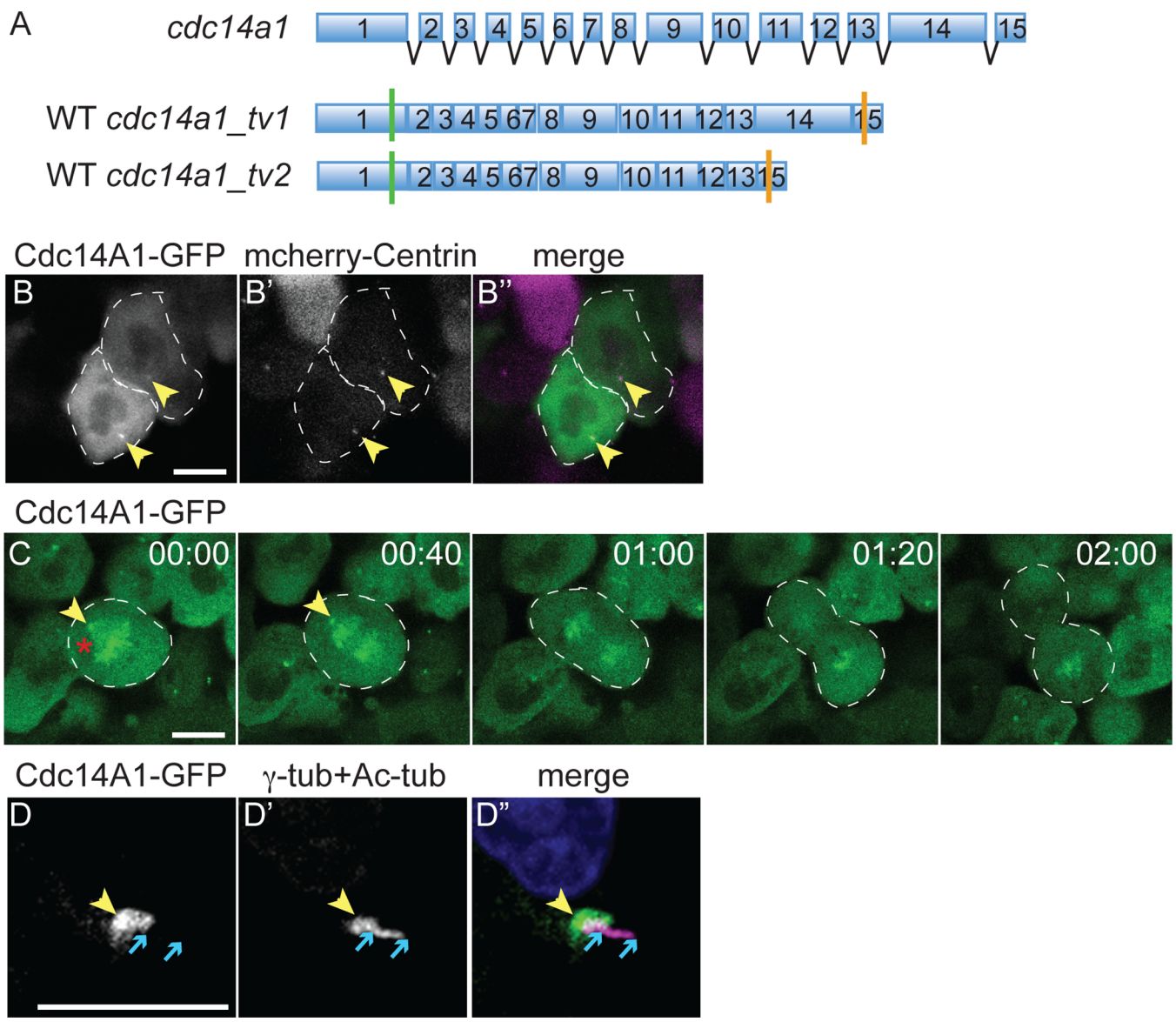

Figure 1. Dynamic distribution of Cdc14A1 during the cell cycle at 8 hpf

A: Structure of *cdc14a1* gene and wild-type (WT) transcripts. Green bars indicate translation start codons and orange bars indicate in frame stop codons. **B–D:** Localization of Cdc14A1 in the ectoderm of live embryos at 8 hpf (B,C) and fixed embryos at 14 hpf (D). (B) The embryo was injected with synthetic *cdc14a1_tv1-GFP* (B, green in B") and mcherry-*centrin* (B', purple in B") RNAs. Dashed lines delimit two cells in interphase. (C) Dividing cell proceeding through metaphase (00:00), anaphase (00:40–01:20) and telophase (2:00). Dashed lines delimit the mitotic cell. (D) The embryo was injected with synthetic *cdc14a1_tv1-GFP* RNA and stained using antibodies against GFP (D, green in D"), γ-tubulin and acetylated tubulin (D', purple in D"). Yellow arrowheads point to the centrosomes. Red asterisk indicates the mitotic spindle. Blue arrows delimit the ends of the cilium. Scale bars represent 10 μm.

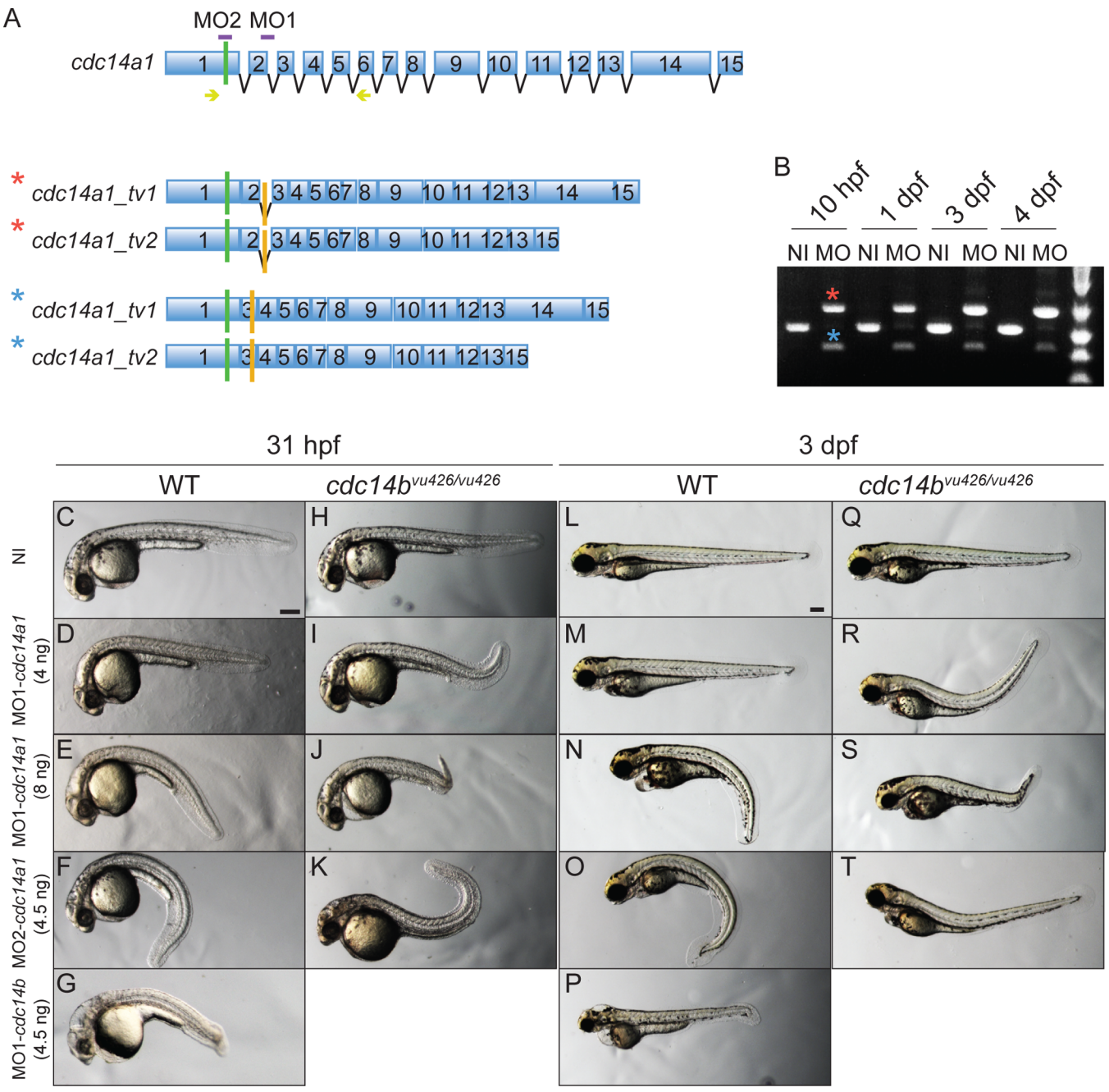

Figure 2. Characterization of *cdc14a1* morphological phenotype

A: Structure of *cdc14a1* gene and aberrant transcripts. Green bars indicate translation start codons and orange bars indicate in frame stop codons. The sequence targeted by each *cdc14a1* MO is indicated in purple. Yellow arrows indicate the sequence of the primers used for RT-PCR in B. **B:** Efficiency of 8 ng MO1-*cdc14a1* over time by RT-PCR. **C–T:** Comparison of morphological phenotypes between non-injected and MO1-*cdc14a1* injected embryos. C,L: non-injected (NI) wild-type (WT) embryos; H,Q: non-injected *cdc14b*$^{vu426/vu426}$ homozygous mutant embryos; D,E,M,N: wild-type embryos injected at the one-cell stage with MO1-*cdc14a1*; F,O: wild-type embryos injected at the one-cell stage with MO2-*cdc14a1*; G,P: wild-type embryos injected at the one-cell stage with MO1-

cdc14b; I,J,R,S: *cdc14b*$^{vu426/vu426}$ homozygous mutant embryos injected at the one-cell stage with MO1-*cdc14a1*; K,T: *cdc14b*$^{vu426/vu426}$ homozygous mutant embryos injected at the one-cell stage with MO2-*cdc14a1*; C–K: embryos at 31 hpf; L–T: embryos at 3 dpf. Scale bar represents 100 μm.

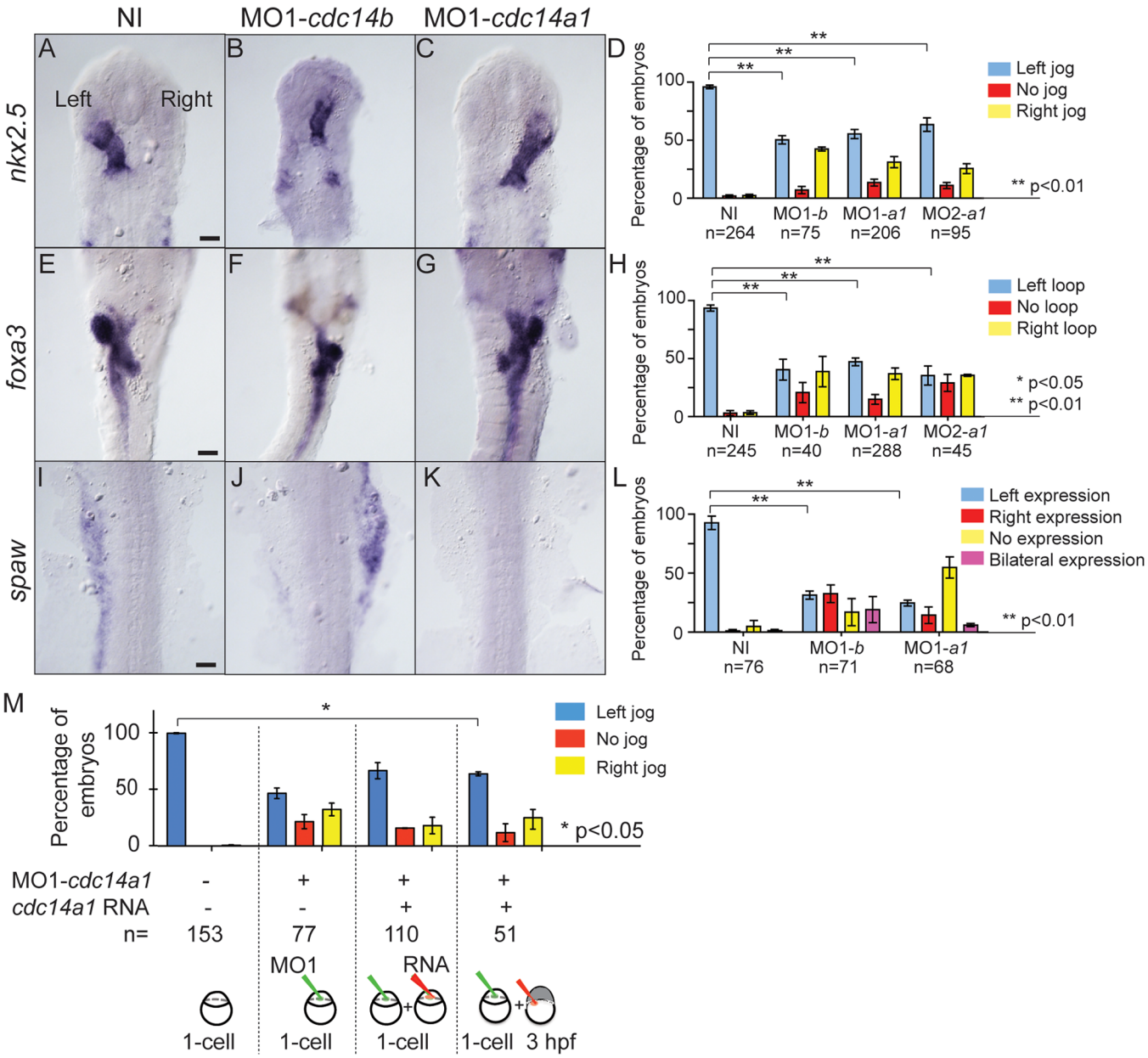

Figure 3. Effect of Cdc14A1 loss of function in LR asymmetry establishment

ISH and expression pattern quantification in non-injected, *cdc14a1* and *cdc14b* MO-injected embryos. **A–D:** *nkx2.5* expression at 31 hpf. **E–H:** *foxa3* expression at 50 hpf. **I–L:** *spaw* expression at 19 hpf. Scale bar represents 100 μm. **M:** Rescue of LR asymmetry defect in Cdc14A1 depleted embryos. Heart tube shifting was determined at 31 hpf. Numbers of embryos analyzed are indicated. Data are represented as mean ± SEM. Statistics were done using Student's *t*-Test (D,H,L) and are only presented for the left sided heart tube class in M.

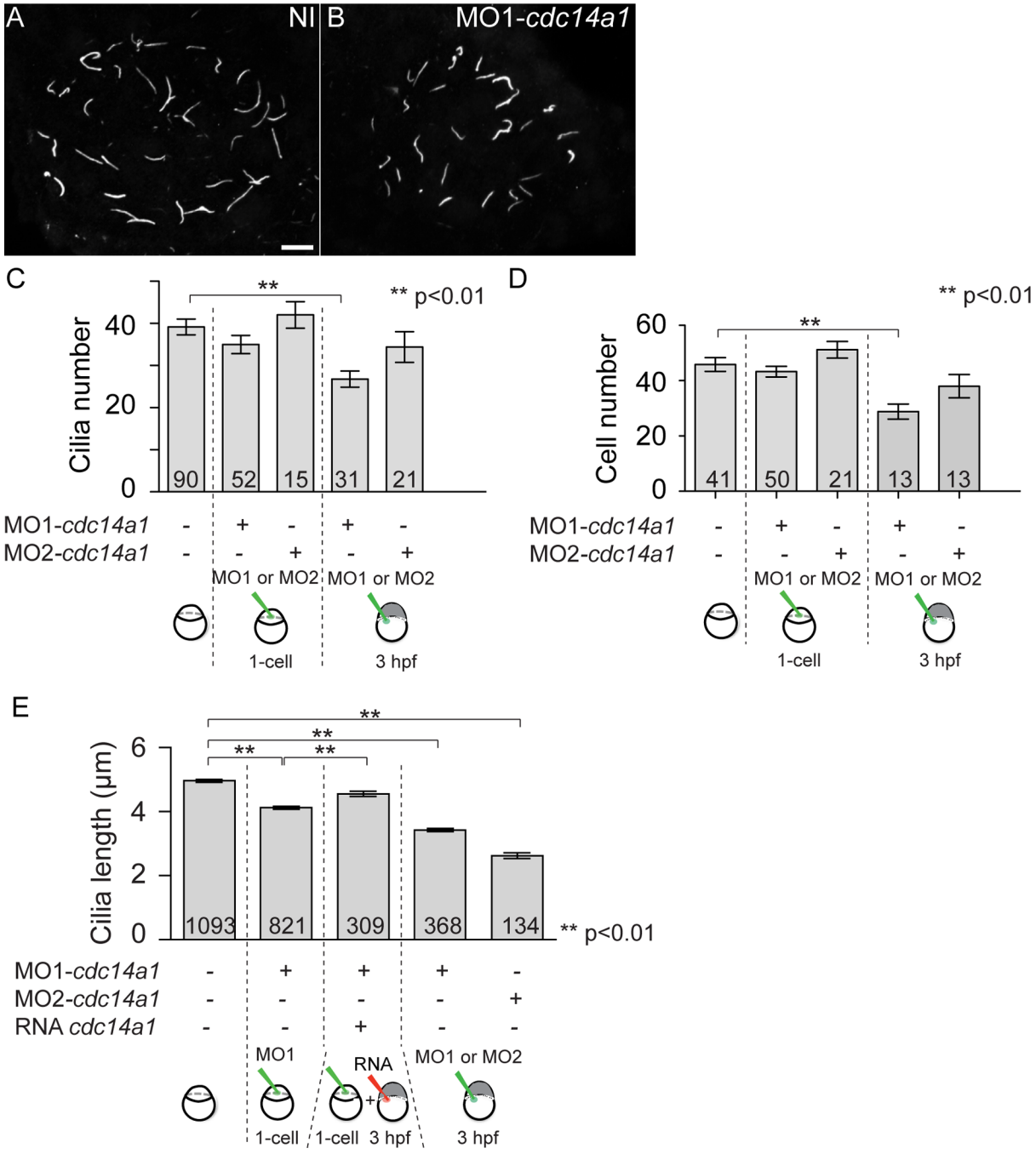

Figure 4. Effect of Cdc14A1 in KV ciliogenesis

A,B: Cilia in the KV at 14 hpf visualized with an anti-acetylated-tubulin antibody. Scale bar represents 10 μm. **C:** Cilia number was determined at 14 hpf. **D:** The number of cells in the KV was determined at 14 hpf. **E:** Cilia length was measured at 14 hpf. The numbers of embryos (C,D) and cilia (E) analyzed are indicated. Data are represented as mean ± SEM. Statistics were done using Student's *t*-Test and calculated against the non-injected sample.

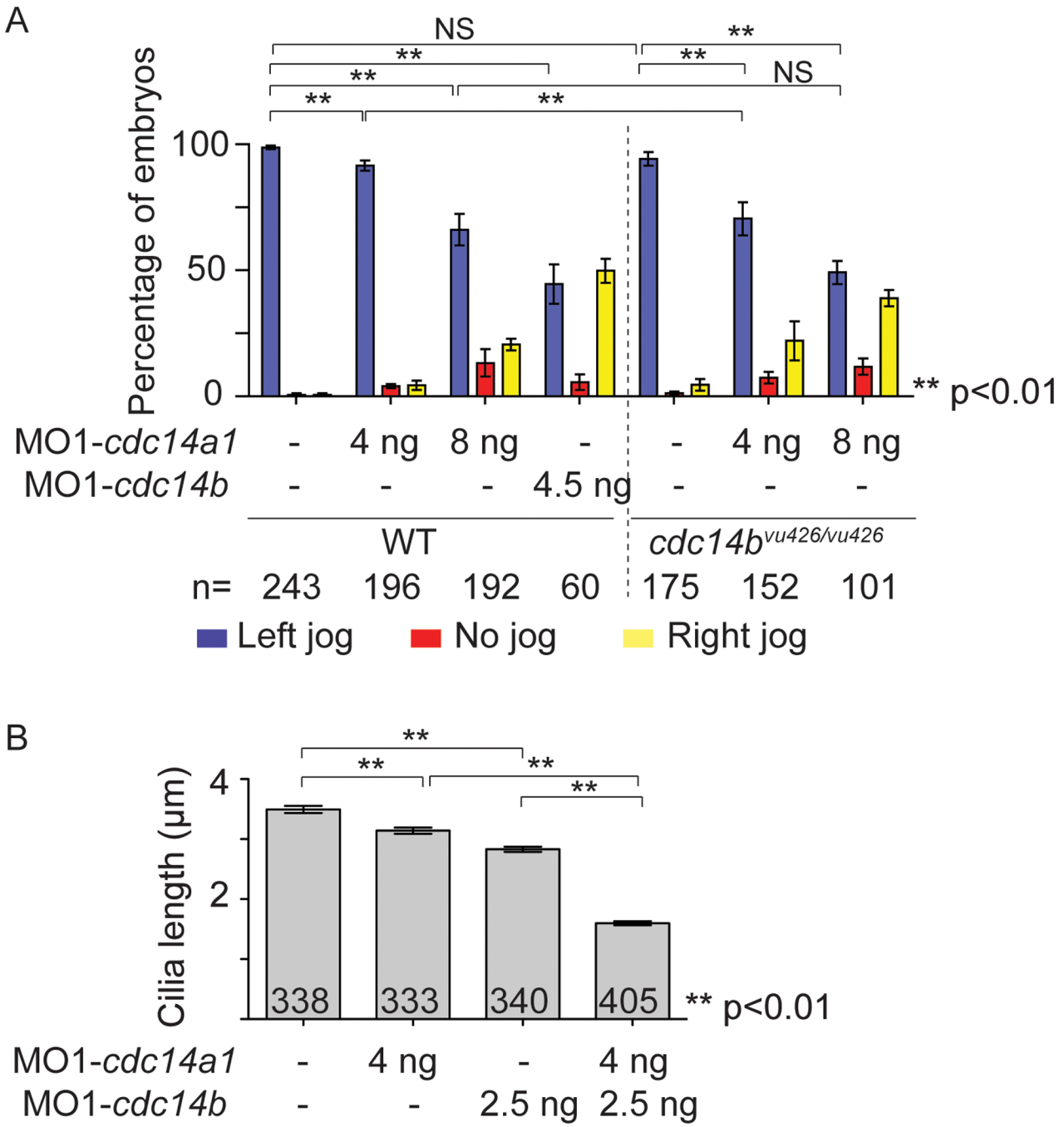

Figure 5. Effect of Cdc14 double loss of function

A: Quantification of heart tube shifting in wild-type (WT) and homozygous *cdc14b*$^{vu426/426}$ mutant embryos non-injected or injected with 4 ng MO1-*cdc14a1*, 8 ng MO1-*cdc14a1* or 4.5 ng MO1-*cdc14b*, at 31 hpf. **B:** Cilia length was measured at 14 hpf. The numbers of embryos (A) and cilia (B) analyzed are indicated. Data are represented as mean ± SEM. Statistics were done using Student's *t*-Test and are only presented for the left sided heart tube class in A.

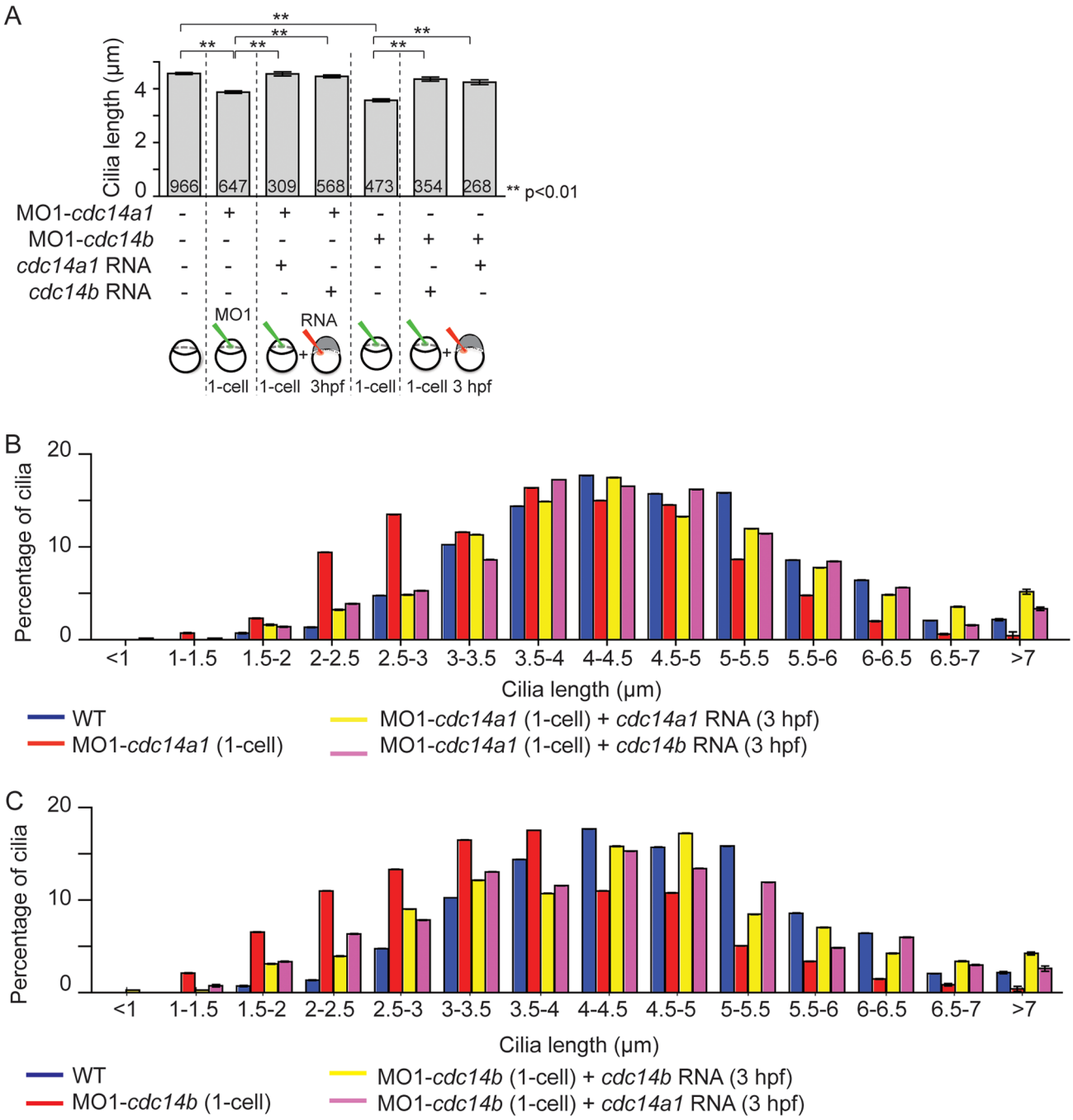

Figure 6. Functional redundancy between Cdc14 proteins

A: Rescue of KV cilia length in *cdc14a1* or *cdc14b* morphant embryos by *cdc14a1* or *cdc14b* RNAs, at 14 hpf. The numbers of cilia analyzed are indicated. Data are represented as mean ± SEM. Statistics were done using Student's *t*-Test. **B:** Graphic representation of the distribution of KV cilia length from (A) in non-injected control, *cdc14a1* morphant and rescued *cdc14a1* morphant embryos. **C:** Graphic representation of the distribution of KV cilia length from (A) in non-injected control, *cdc14b* morphant and rescued *cdc14b* morphant embryos.